

COTR AND SASE GENERATED BY CHICANE-COMPRESSED ELECTRON BEAMS

A.H. Lumpkin, Fermilab*, Batavia, IL U.S.A. 60510

R.J. Dejus and N.S. Sereno, Argonne National Laboratory, Argonne, IL U.S.A. 60434

ABSTRACT

Observations of strongly enhanced optical transition radiation (OTR) following significant bunch compression of photoinjector beams by a chicane have been reported during the commissioning of the Linac Coherent Light Source (LCLS) accelerator and recently at the Advanced Photon Source (APS) linac. These localized transverse spatial features involve signal enhancements of nearly a factor of 10 and 100 in the APS case at the 150-MeV and 375-MeV OTR stations, respectively. They are consistent with a coherent process seeded by noise and may be evidence of a longitudinal space charge (LSC) microbunching instability which leads to coherent OTR (COTR) emissions. Additionally, we suggest that localized transverse structure in the previous self-amplified spontaneous emission (SASE) free-electron laser (FEL) data at APS in the visible-UV regime as reported at FEL02 may be attributed to such beam structure entering the FEL undulators and inducing the SASE startup at those structures. Separate beam structures 120 microns apart in x and 2.9 nm apart in wavelength were reported. The details of these observations and operational parameters will be presented.

PACS: 41.60.Ap, 41.60.Cr

*Work supported by U.S. Department of Energy, Office of Science, Office of High Energy Physics, under Contract No. DE-AC02-06CH1135

I. INTRODUCTION

Several years ago the self-amplified spontaneous emission (SASE) free-electron laser (FEL) experiments [1] at the Advanced Photon Source (APS) included a series of observations on z -dependent microbunching as measured by visible light coherent optical transition radiation (COTR) [2-4]. This SASE-induced microbunching (SIM) exhibited clear spectral effects at the fundamental and second harmonic of the FEL wavelength. The z -dependent gain of the COTR was comparable to that of the SASE as expected. At the International FEL Conference in 2002 the authors of reference 5 reported localized spatial enhancements of the COTR images, and in fact reported two 250- μm FWHM clusters 120- μm apart and different in wavelength by 2.9 nm in images taken after undulator #6 of a string of 9 as shown in Fig. 1. At that time it was proposed that there must be localized structures in the electron beam distribution generated perhaps in the chicane that the SASE process preferentially selected. Originally, the investigators checked the e-beam emittance with YAG:Ce screens located after the chicane. Some intensity variations of 10-20% across the profile were seen, but it was not clear those fluctuations were enough to be selected preferentially by the SASE process. (The YAG:Ce scintillation strength would have masked the COTR effects to a large extent.)

As it was understood at that time, there was no theory that supported the coherent synchrotron radiation (CSR) microbunching instability's extending to visible wavelengths in the linac [6, 7]. Subsequently, it was proposed that the LSC fields might be the main effect in driving the microbunching instability at FIR wavelengths in a linac [8, 9]. We now propose that the LSC-CSR microbunching instability in the linac at 300-A peak current had effected the observed spatially localized SASE-induced microbunching and related SASE effects in the visible light regime in those 2001 experiments at APS. We report the new evidence for this connection. We have reviewed the archived data taken at an optical transition radiation (OTR) screen just before and after the first undulator, and strong, spatially localized enhancements are clear in the 300-A

data. These are comparable to the Fig.1 spatial structures seen after undulator 6. More recently, “unexpected” enhancements of the signals in the visible light-IR OTR monitors (CCD cameras) were observed after compression in a chicane bunch compressor at LCLS [10] and APS [11].

II. EXPERIMENTAL BACKGROUND

The measurements were performed at the APS facility which includes an injector complex with two thermionic cathode (TC) rf guns for injecting an S-band linac that typically accelerates the beam to 325 MeV, the particle accumulator ring (PAR), the booster synchrotron that ramps the energy from 0.325 to 7 GeV in 220 ms, a booster-to-storage-ring transport line (BTS), and the 7-GeV storage ring (SR). In addition, there was an photocathode (PC) rf gun that could also be used to inject into the linac and to ultimately provide beam to the FEL as shown schematically in Fig. 2. An extensive diagnostics suite is available in the chicane and after the chicane area as described in reference 11. The microbunching instability tests were performed in the linac at the three imaging stations after the chicane bunch compressor and at the end of the linac where another beam imaging station is located. A FIR coherent transition radiation (CTR) detector (Golay cell) and Michelson interferometer are located between the three-screen emittance stations. This system is described in more detail elsewhere [12].

The YAG:Ce emissions and OTR were directed by turning mirrors and relay optics to a Pulnix CCD camera located 0.5 m from the source. These Chicane stations also have options for low- and high-resolution imaging of the beam spot by selecting one of two lens configurations [13]. The near-field, low-resolution magnification resulted in calibration factors of 48.8 μm per pixel in x and 38.9 μm per pixel in y. The OTR signal strength with a 400-pC micropulse was too low to use the high-resolution mode. The signal intensity was adjusted with a remotely-controlled iris (with no absolute position readback) in the path to the camera. The OTR and YAG:Ce images were recorded by a Datacube MV200 video digitizer for both online and offline image analyses, and a video switcher was used to select the camera signal for digitizing.

At the end of the linac, the imaging station included the optical transport of the visible light out of the tunnel to a small, accessible optics lab where the Vicon CCD camera was located. This allowed the access for manually inserting bandpass (BP) filters and neutral density (ND) filters in front of the camera to assess the spectral dependency of the enhanced OTR. A set of BP filters with center wavelengths in 50-nm increments from 400 to 750 nm and 40-nm band width as well as a 500-nm shortpass filter and 500-nm long pass filter were used in the initial tests [11]. However, recently the Oriel spectrometer and readout cameras were moved from the FEL hall to this station to extend our spectral analysis capabilities for the LSC-induced microbunching (LSCIM) COTR effects. The beam energy was 325-375 MeV at this station in these recent experiments.

The YAG:Ce (Y0-9) stations and the visible light diagnostics (VLD0-9) stations in the FEL are schematically shown in pairs in Fig. 2 with a detailed view in Fig. 3. They were designed to assess the z-dependent SASE evolution with both near-field and far-field imaging optics and to track the e-beam position and size through the undulator string. They included the filter wheels that allowed the remote selection of ND filters and BP filters for insertion in the radiation path to the cameras. They were augmented to provide an OTR/blocking foil at the first YN actuator. This foil was used to prevent the SASE and SER from reaching the second, retractable pickoff mirror oriented at 45 degrees to the beam direction and 63 mm downstream of the first actuator. This configuration was used in the first SIM COTR experiments in the visible regime [2,3] at this downstream portion of the station. The data being reassessed are from a comprehensive set of SIM tests at two peak currents, 120 A and 300 A, taken on December 20, 2001. The VLD0 station is before the first undulator and provides the key OTR images at the two currents. Evidently the threshold for seeing the LSCIM COTR effects in the visible regime was passed at the higher peak current with 2.5 times more compression.

III. RECENT CTR and COTR RESULTS

The more recent experiments [11] were initiated by transporting the PC gun beam accelerated to 150 MeV to the chicane area. The rf phase of the L2 accelerator structure located before the chicane was used to establish the appropriate conditions for compression in the chicane. The degree of compression was tracked with the Golay cell signals. A very strong variation of the FIR signal with L2 phase was observed as shown in Fig. 4. There were only a few units of CTR signal seen with the beam uncompressed and 300 units seen at the peak compression. The autocorrelation scan was then done and showed a profile width of $\sim 65 \mu\text{m}$ (FWHM). This would mean a roundtrip time of $130 \mu\text{m}$, or about 430 fs (FWHM). The initial UV drive laser pulse was 3 to 4 ps (FWHM) as determined by an autocorrelator.

Having determined we had maximum compression from the Golay-cell data, we then sampled the beam images at the three screens after the chicane in the emittance measurement area. The sample shown is from FS5, the third screen of the set. At the point of minimum compression the OTR image is dim, and visibly tilted in x-y space. In contrast, the image taken near full compression (as indicated by the FIR CTR signal) has significantly enhanced localized spikes of about $250 \mu\text{m}$ (FWHM) spatial extent as shown in Fig. 5. The pseudo-color intensity scale at the right of the image shows that the red areas are high intensity. The profile in Fig. 5b shows the peak intensity of 180 counts, almost 10 times the adjacent intensities in the beam-image footprint. We do not see the ring-like structure in the enhancement reported at LCLS [10], but we also don't have a harmonic cavity for linearizing longitudinal phase space before the chicane as LCLS has. On this particular run, we noted that there was a preferred location in the footprint to be enhanced. The enhanced vertical band in Fig. 5a is the same area that shows less enhancement with less compression.

An additional indication of the effect is shown in Fig. 6, where the peak intensities from the vertical profiles taken through the images at each phase setting show the rapid increase in the

enhanced OTR signal in just a few degrees of L2 phase change. The order of magnitude enhancement is clearly seen in this plot. A similar plot for horizontal profiles was done, and this showed a slight shift of the intensity peak compared to the CTR data by 0.4 degrees in L2 phase. Integrated areas of the ten images at each phase setting do not show this degree of enhancement, but about a 1.6 to 2 times larger counts integral at peak compression was seen with larger fluctuations in the compressed conditions. This fact is consistent with the premise that the charge transport efficiency is not the cause of the effect nor CSR-induced clumping of electrons, but rather a coherent enhancement of some kind is involved.

In order to assess the spectral dependency of the OTR enhancements, we accelerated the beam to 375 MeV and again imaged the beam spot with OTR at a downstream station. As described previously, this station included transport of the signal outside of the tunnel to a small optics lab. First, we still see enhanced localized spikes when we have compressed the beam as shown previously [11]. In this case enhancements of the OTR signals when at maximum compression are about 3-6 times the normal intensity. The strong fluctuations of these enhanced areas are again suggestive of a coherent process seeded by noise.

At full compression we checked the spectral dependency of the enhancements by inserting the BP filters in front of the CCD camera. Our initial results are that the enhancements were seen at all central wavelengths from 400 to 750 nm (in steps of 50 nm), although much weaker in the 400 to 500-nm regime than at 550 nm. We subsequently checked the spectral dependence of incoherent OTR from the TC gun beam and saw an intensity roll off in this shorter wavelength interval which we can attribute partly to the standard manufacturer's CCD camera response curves for these different wavelengths [14]. However, this rolloff was not as much as the observed COTR intensity rolloff [15,16]. We also saw relatively more enhancement of intensity in the 500-nm longpass filter data than in the 550-nm shortpass filter data.

Additionally, in Fig. 7 we show our initial results from the spectrometer when positioned at a station at the end of the linac. The YAG:Ce light in Fig. 7a peaks at about 530 nm and shows the full spatial x size of the beam as about 5 mm in the vertical display axis. The broadband spectral streaks originate from localized x structures (sub-200 μm) which appear with bunch compression in both cases. The YAG:Ce screen setup uses an Al mirror at 45 degrees to the beam to direct the light to the camera. This mirror is in the same plane as the OTR converter mirror when it is inserted so we can detect COTR from it as well. The spectrometer entrance slit was opened to 2000 μm to facilitate the first data acquisition so the spectral resolution was broadened to about 40 nm. In subsequent experiments with an ICCD readout camera, we were able to narrow the entrance slit and obtain few-nm resolution [15,16].

IV. PAST OTR, COTR, and SASE RESULTS with PC rf GUN BEAMS

The purpose of this section is to introduce experimental evidence for enhanced OTR attributable to LSC-induced microbunching. We are now able to connect our Dec. 2007 LSCIM COTR data with an original series of experiments that were performed on Dec. 20, 2001. The objectives then were to explore the SASE-induced microbunching in the FEL as probed with COTR-based techniques using near-field focusing. In addition, we used a 500-nm short pass filter to exclude the 530-nm fundamental SASE or COTR in the low gain region to check the incoherent broadband image. The beam energy was 217 MeV. Now this filter also lets us look for enhancements that are not SASE induced. In this particular run we only had one filter available with a factor of about 100 rejection ratio for wavelengths longer than 500 nm, so we cannot rely on this to completely reject the SASE-induced contributions after several gain lengths along z. We took data at both 120 A and 300 A peak current. The beam parameters are shown in Table 1 [5]. The comprehensive test series also included z-dependent gain measurements of both COTR and SASE including the critical VLD0

reference data taken just *before the first undulator*. In Fig. 8 we show the beam image from VLD0 at 120 A. It is a relatively weak OTR image with 450 pC of charge. This is compared to a sample image from VLD0 in the 300-A run which clearly has localized spatial enhancements in it as shown in Fig. 9. The same color intensity scale is used, and we added ND 0.5 in the 300-A case to avoid camera saturation. The peaks of Fig. 9 are thus 5-6 times stronger than the 120-A case peak in Fig. 8. The 100-image integrated intensity averages were 2 times stronger in the 300-A case than the 120-A case for very similar micropulse charge. These results are clear evidence for a coherent enhancement of some kind which we now attribute to the LSC microbunching instability and subsequent visible light COTR emissions. (We note that we have recently re-commissioned the VLD0 station, transported compressed PC-gun beam to this station, and again observed L2 phase effects on the observed COTR intensity. This test clearly links the two experimental eras.)

We then checked that after one undulator the enhancements persist in the 500-nm shortpass data from VLD1 as shown in Fig. 10a. Of course, we cannot take simultaneous data sets so this is a different beam micropulse, but the effect remains. The intensity scale on the right provides the factor of 5 ratio of the peaks to base intensity. In addition, in Fig.10b we show the SIM+LSCIM COTR image taken with a single ND1.0 filter whose peaks are thus about 5 times stronger than those of filtered LSCIM-only images. The localized spatial structures in the LSCIM image are enhanced in intensity in the SIM COTR images. This is particularly true in the VLD2 images where the right hand peak was ~ 100 times brighter than the shortpass-filtered data. Again such examples are representative of the 100 images taken in each configuration. This is strong evidence for our hypothesis on SASE startup being favored at the localized LSCIM structures.

For comparison and perspective purposes the z-dependent gain curves for the COTR and SASE for the 300-A cases are shown in Figs. 11 and 12, respectively, and compared to GENESIS calculations. The GENESIS calculations used the 300-A parameter set from Table 1. The COTR

data clearly have a faster startup in the VLD1-2 region than the GENESIS curve and saturate after undulator 4 at $z \sim 10$ m in Fig. 11. Since there was an rf power trip in the linac during the z scan after the VLD4 data were taken and only 87% charge transport was regained, a second GENESIS run was done with 260-A peak current. In these two cases, the GENESIS-calculated microbunching fraction squared is plotted which should scale like SIM COTR. The COTR data are the most direct measure of the microbunching evolution at the SASE fundamental wavelength since the foils sample at discrete z locations. The saturated power level of the 260-A run falls closer to the data curve. There are three SASE gain curves shown in Fig.12 which saturate at about undulator 5; one experimental curve with 100-image region-of interest (ROI) averages taken at each location for decreasing undulator number, and two from the GENESIS [17] simulations recently done for 300-A and 260-A peak current. In this figure the GENESIS curves were also normalized to the undulator 1/VLD1 data location. The experimental curve and GENESIS overlap up to VLD2, and then the simulation curve is seen *above* the data in the VLD3,4 area. The combined COTR and SASE comparisons are consistent with the hypothesis of there being extra microbunching contributions beyond the SIM source as viewed through COTR. Due to possible trajectory effects on the gain curve, these cases can be viewed as a scenario consistent with the proposed startup effect due to LSC-related microbunching.

COTR and SASE: Imaging Spectrometer Results

Having demonstrated that the localized structures are present after VLD0 and VLD1 with 300-A beam, we still need to check that they are also present in the VLD6 data that complement the COTR-6 spectrometer data. In Figs.1, 13 we show the $x-\lambda$ images, one published in ref. 5 and one now just being reported. Both of these, as well as many other images taken at that time, show the localized spatial structures. The x-axis is on the vertical display axis. In Fig. 13 the two

enhancements are ~ 150 μm apart in x and ~ 3 nm apart in wavelength near the nominal 530-nm SASE fundamental wavelength. These data were recorded after SASE saturation occurred.

Further review of the old data sets led to the finding of the SASE x - λ data shown in Fig. 14. There is structure on the x direction in the vertical display axis. Since physically the spectrometer slit is along this direction, we do not believe this spatial intensity modulation is a diffraction effect from that particular slit. This feature needs additional review of other images and stations.

Discussion

We had identified several characteristics of the enhanced OTR signals that were used to evaluate which mechanism was involved [11]. If we consider charge transport efficiency, radiation enhancements, and spectral structure observed, we can discriminate among microbunching, a longitudinal spike with a sharp leading edge, multiple submicron spikes, and CSR-induced clumping. We initially considered whether there were microbunching from the drive laser interaction with the low-energy photoelectrons such as found under high laser power conditions, but a simple calculation of the laser field strengths showed this effect would not be measurable [11]. Since the transported charge through the chicane and undulators in the past was constant to 10% during the phase scan, we cannot explain the large, localized spatially OTR enhancements as only due to CSR-induced clumping of the charge distribution. Assuming the clumping does not involve microbunching, there would be no way to explain the observed OTR enhancements of the total image intensities by factors of two or more. Finally, our initial spectral sampling across the visible light region with 40-nm band widths showed a broadband character like that of incoherent OTR, but the COTR was relatively red enhanced [16]. Additionally, in Fig. 7 we show our initial results from the spectrometer (with CCD readout) when positioned at a station at the end of the linac. The broadband streaks clearly originate from the localized x structures which appear with bunch

compression. Such post-chicane data are consistent with coherent enhancements of wavelengths longer than a fine longitudinal structure, such as a leading-edge spike. However, a recent report by Z. Huang [18] also shows a broadband enhancement in the visible regime due to the LSC instability and the chicane compression process. We suggest another discriminating test is whether LSC-induced microbunching would act as “localized prebunched beam” and induce startup of visible wavelength SASE FELs at these structures, and that aspect is what was actually reported six years ago in the FEL02 transverse-dependencies paper [5].

V. SUMMARY

In summary, we have connected for the first time the previously reported transverse dependencies on SIM COTR of FEL02 with broadband LSCIM effects as identified in investigations described over the last year. This key identification was based on a revisit and interpretation of the 300-A data taken at ANL in 2001. Common to these two sets of ANL data are the laser, photocathode material, the linac, the chicane, and the optical spectrometer. The PC rf gun cavities are different with different transverse emittances, but similar longitudinal emittances. We will be reviewing other data sets from past ANL visible, UV, and VUV SASE experiments as time permits. Start-to-end simulations would be welcomed that investigate this proposed connection of LSCIM and SASE startup. The growing interest in these COTR effects is indicated by the time allowed for discussion in the recent high-brightness beams workshop at Zeuthen in May 2008 [19] and the Microbunching Instability Workshop II in October 2008 at Berkeley [20]. It remains to be confirmed if this LSC microbunching instability played, or will play, a role in FEL startup in the optical and infrared regime of other experiments.

VI. ACKNOWLEDGEMENTS

The authors acknowledge support from M. Wendt of Fermilab and R. Gerig, K.-J. Kim, and H. Weerts of the Argonne Accelerator Institute. We acknowledge Y.-C. Chae for providing the new GENESIS simulations. We acknowledge discussions with K.-J. Kim, Y.-C. Chae, and M. Borland of Argonne National Laboratory; Z. Huang of SLAC; A. Gover of the Univ. of Tel Aviv; and W. Fawley of LBNL. They also acknowledge W. Berg and S. Shoaf of Argonne National Laboratory for the recent relocation of the optical spectrometer and cameras with controls to the small diagnostics lab linked to linac Sta-5.

Table 1: Summary of the beam parameters for uncompressed and compressed states in the previous COTR and SASE tests at 530 nm performed on December 20, 2001 [5].

Parameter	Uncompressed	Compressed
Beam Energy (MeV)	217 MeV	217
Emittance x (mm mrad)	4.6 after chicane	4.1 after chicane
Emittance y (mm mrad)	4.3 after chicane	4.2 after chicane
Peak Current (A)	120	300
Bunch Length (ps rms)	1.6	0.65
Charge (pC)	450	450
Energy Spread (%)	0.1-0.2	< 0.1

REFERENCES

- [1] S.V. Milton et al., *Science* **292**, 2037 (2001).
- [2] A.H. Lumpkin et al., “First Observation of z-dependent Microbunching using Coherent Transition Radiation,” *Phys. Rev. Lett.*, Vol. 86(1), 79, January 1, 2001.
- [3] A.H. Lumpkin et al., “First Observations of Micro-bunching “Sidebands” in a Saturated FEL Using Coherent Optical Transition Radiation”, *Phys. Rev. Lett.*, Vol. 88, No. 23, 23480101-1, June 10, 2002.
- [4] A.H. Lumpkin et al., “First Observations of Electron-Beam Microbunching in the Ultraviolet At 265 nm Using COTR in a SASE FEL”, *Nucl. Instr. and Method*, A483, 402-406, (2002).
- [5] A.H. Lumpkin et al., “Evidence for Transverse Dependencies in COTR and Microbunching in a SASE FEL”, the Proc. of the 23rd FEL Conference, Argonne, Il, Sept.9-13, 2002. *Nucl. Instr. and Meth. A* 507, 200-204, (2003).
- [6] M.Borland et al., *Nucl. Instr. Methods Phys. Res. Sect. A* **483**, 268 (2002).
- [7] E.L. Saldin, E.A. Schneidmiller, and M.V. Yurkov, *Nucl. Instr. Methods Phys. Res. Sect. A* **490**, 1 (2002).
- [8] E.L. Saldin, E.A. Schneidmiller, and M.V. Yurkov, DESY Report No. TESLA-FEL-2003-02, 2003.
- [9] Z. Huang et al., *PRST-AB* **7**, 074401 (2004).
- [10] D.H. Dowell et al., “LCLS Injector Commissioning Results”, Proc. of FEL07, Aug. 26-30, 2007, Novosibirsk.
- [11] A.H. Lumpkin et al., “Observations of Enhanced OTR Signals from a Compressed Electron Beam”, submitted to the Proc. of BIW08, Tahoe, Ca , May 5-8, 2008

- [12] A.H. Lumpkin et al., “Initial measurements of CSR from a Bunch-Compressed Beam at APS.”
Proc. of FEL05, JACoW/eConf C0508213, 608 (2005).
- [13] B.Yang et al., “Design and Upgrade of a Compact Imaging System for the APS Linac Bunch Compressor”, BIW2002, AIP Conf. Proc. 648, 393 (2002).
- [14] For example the CCD sensitivity charts on www.jai.com which include Pulnix cameras.
- [15] A.H. Lumpkin et al., “Spectral and Charge-dependence Aspects of Enhanced OTR Signals from a Compressed Electron Beam”, submitted to the Proc. of Linac08, Victoria, B.C. September 28-Oct.3, 2008.
- [16] A.H. Lumpkin, R.J. Dejus, N.S. Sereno, “Characterization and Mitigation of COTR Signals from Chicane-compressed Electron Beams”, submitted to Phys. Rev. ST-AB, January 2009.
- [17] S. Reiche, Nucl. Instrum. Methods Phys. Res., Sect A **429**, 243 (1999).
- [18] Z. Huang et al., “COTR and CSR from Microbunched LCLS Beam”, Mini Workshop on “Characterization of High Brightness Beams”, Zeuthen, Germany, May 26-30, 2008.
- [19] Agenda for Mini Workshop on “Characterization of High Brightness Beams”, Zeuthen, May 26-30, 2008.
- [20] Agenda for Microbunching Instability Workshop II, Chairman W.M. Fawley, LBNL, Berkeley CA, October 6-8, 2008.

FIGURE CAPTIONS

Figure 1: An example of the imaging spectrometer data after undulator 6 showing the COTR x - λ dependence at ~ 530 nm first reported at FEL02 [5].

Figure 2: A schematic of the APS linac test area showing the PC rf gun, the TC rf gun, the accelerator structures, the chicane, the decommissioned FEL with VLD stations after each of nine undulators, the imaging optical spectrometer, and the electron beam dump circa 2001 (ref. 5).

Figure 3: A schematic of the YN and VLDN stations located before the first undulator and after each of the nine undulators at the time of the SASE-induced COTR experiments.

Figure 4: FIR CTR signal from the Golay cell variation with the upstream L2 phase in degrees.

Figure 5: OTR beam image (a) and horizontal profile (b) through spike in distribution after the Chicane with L2 phase = 14.9 degrees, close to maximum compression [11].

Figure 6: Plot of the peak intensities from the OTR image vertical profiles taken near the enhanced regime coordinates as a function of L2 phase in degrees [11].

Figure 7: Example x - λ images of the present PC gun beam at 375 MeV near maximum bunch compression for a) YAG:Ce screen plus “COTR streak” and b) the COTR screen only. In this case the 95 lines/mm grating was selected in the spectrometer, and the wavelength span is about 180 nm. The broadband emission streak is clearly from a localized x location in both images.

Figure 8: An example of VLD0 OTR data with the 120-A beam and 450-pC micropulse with ND 0.0.

Figure 9: An example of VLD0 OTR/COTR data with the 300-A beam and 450-pC micropulse with ND 0.5.

Figure 10: Two examples of VLD1 OTR/COTR data with the 300-A beam for a 450-pC micropulse: a) The image with 500-nm shortpass filter that blocks most 530-nm SASE-related

COTR. (There are two distinct peaks shown attributed to LSCIM) and b) The SIM +LSCIM COTR image with ND1.0 filter and no shortpass filter. One sees a similar two peaks, but with about 5 times more intensity.

Figure 11: The z-dependent COTR gain curve a) for SASE-induced microbunching at the FEL fundamental wavelength of 530 nm on December 21, 2001 and for recent GENESIS simulations of the microbunching fraction squared for b) the 300-A case and c) the 260-A case.

Figure 12: The z-dependent gain curve a) for SASE at 530 nm taken by stepping through the nine VLD stations in decreasing order for data set 5 and for GENESIS simulations done for beam parameters for b) the 300-A case and c) the 260-A case.

Figure 13: Another example of the imaging spectrometer data showing the COTR x - λ dependence near the 530-nm fundamental wavelength after undulator 6 from Dec. 20, 2001 experiments.

Figure 14: An example imaging spectrometer image of undulator radiation sampled after undulator 6 with the 300-A beam from Dec. 20, 2001. Localized spatial spikes are evident on the vertical display axis which is the x spatial axis.

FIGURES

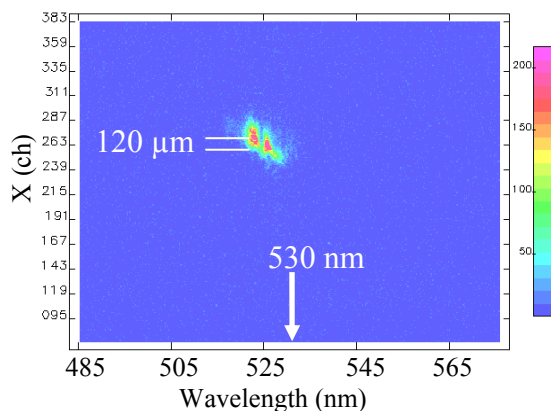


Fig. 1

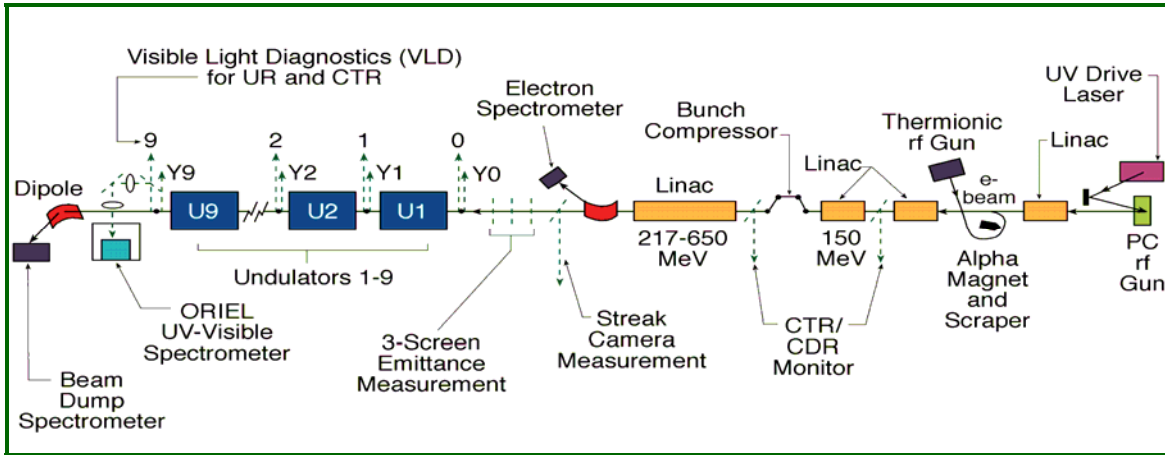


Fig. 2

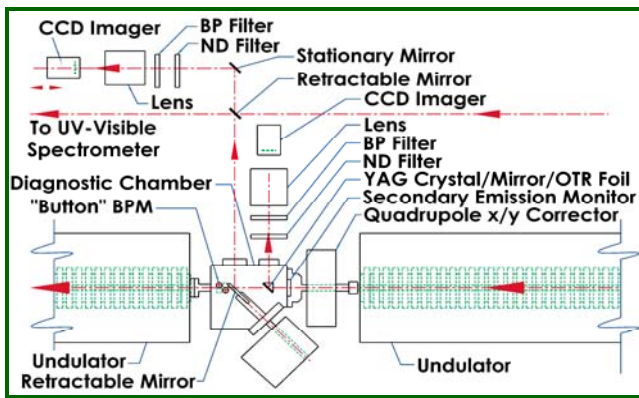


Fig. 3

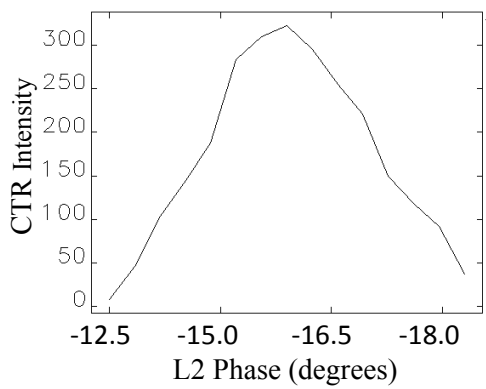


Fig. 4

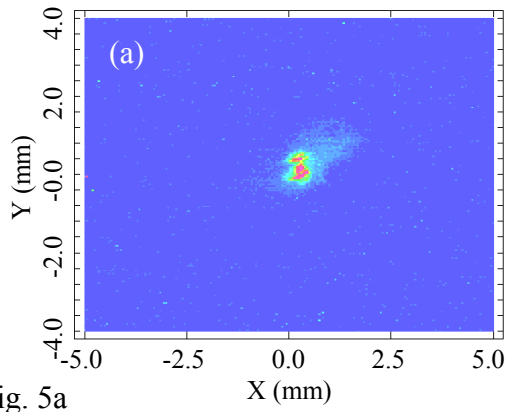


Fig. 5a

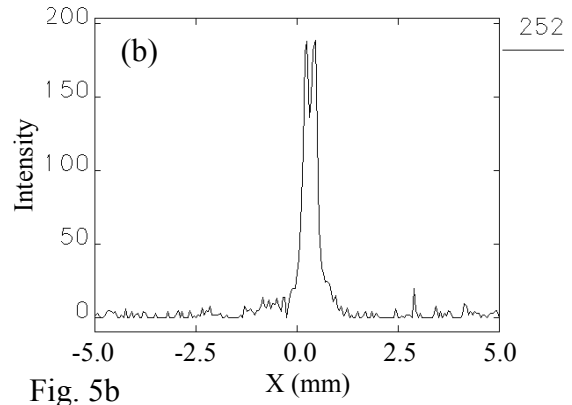


Fig. 5b

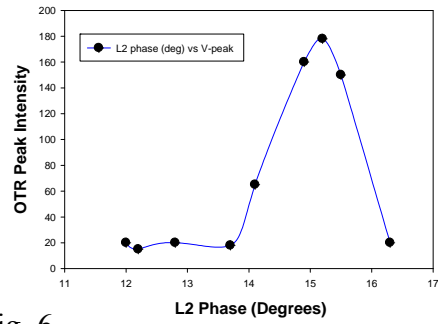


Fig. 6

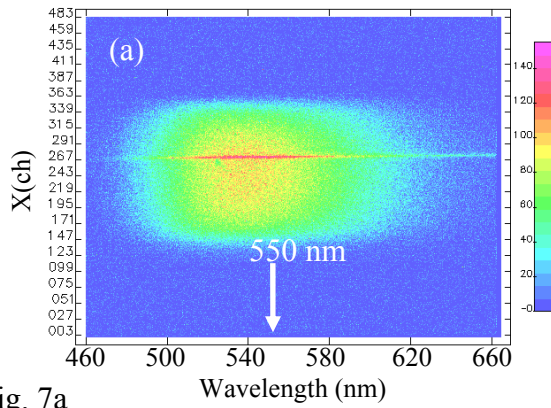


Fig. 7a

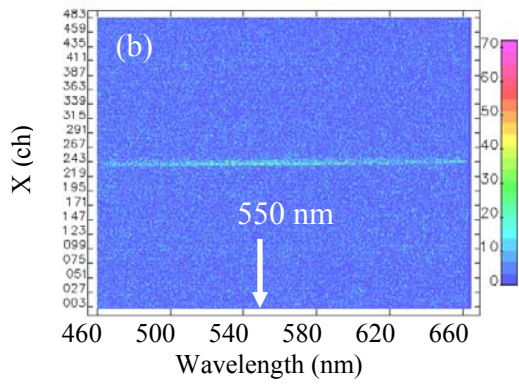


Fig. 7b

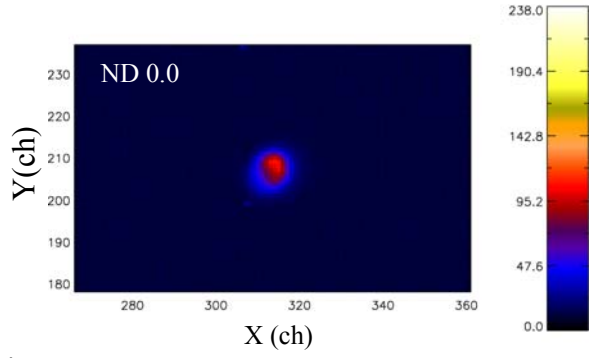


Fig. 8

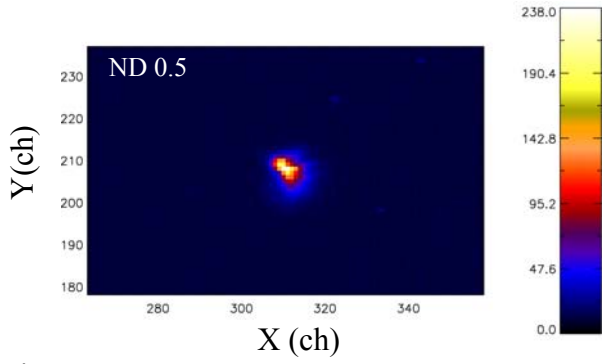


Fig. 9

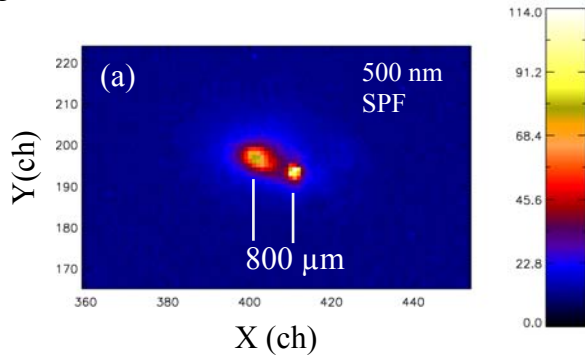


Fig. 10 a

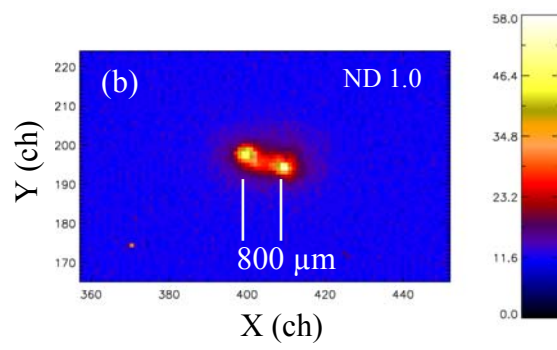


Fig. 10 b

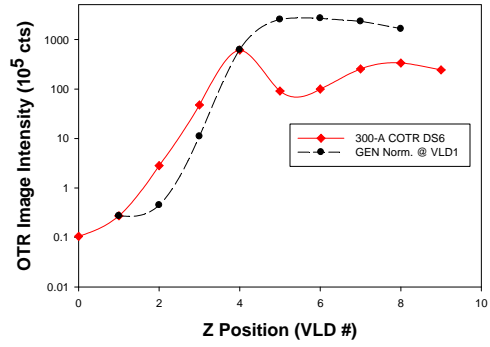


Fig. 11

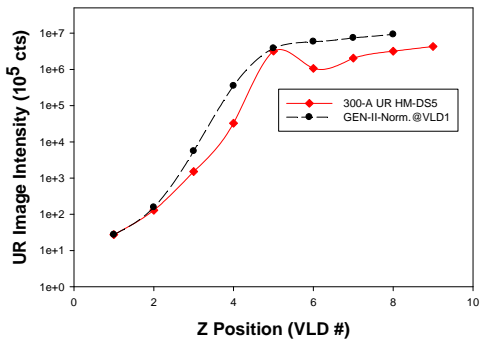


Fig. 12

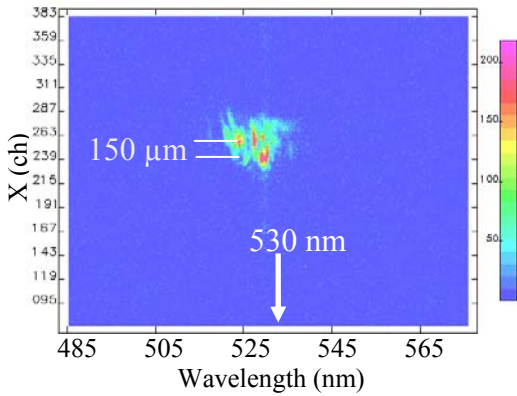


Fig. 13

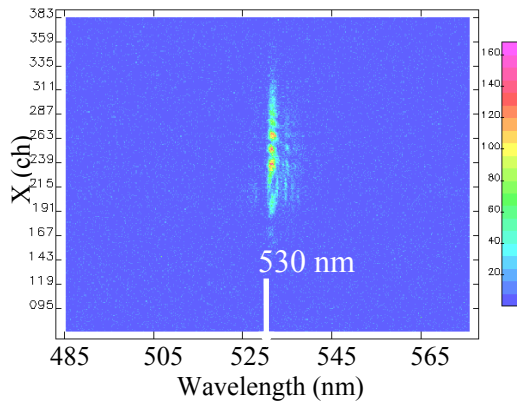


Fig. 14